Enhancement of the photocatalytic activity of decatungstate, W10O324–, for the oxidation of sulfasalazine/sulfapyridine in the presence of hydrogen peroxide

P. Cheng, Yajie Wang, M. Sarakha, Gilles Mailhot

Enhancement of the photocatalytic activity of Decatungstate, $W_{10}O_{32}^{4-}$, for the oxidation of sulfasalazine/sulfapyridine in the presence of hydrogen peroxide

P. Cheng[1], Yajie Wang[2], M. Sarakha[1]*, G. Mailhot[1]

[1]Université Clermont Auvergne, CNRS, Sigma Clermont, Institut de Chimie de Clermont Ferrand (ICCF) UMR 6296, BP 80026, F-63171, Aubière cedex, France.
[2]School of Eco-Environmental Engineering, Guizhou Minzu University, Guiyang 550025, China
*** Corresponding author**

Abstract

The degradations of sulfasalazine and also sulfapyridine have been investigated by using the sodium decatungstate $Na_4W_{10}O_{32}$ as a photocatalyst in the presence of hydrogen peroxide as a sacrifial agent. The selective irradiation of decatungstate, $W_{10}O_{32}^{4-}$, in the presence of the pollutants at 365 nm and at pH = 4.0 leads to the reduction of hydrogen peroxide via a Fenton like reaction involving the reduced species, $W_{10}O_{32}^{5-}$. Such process represents an efficient way for the formation of the highly reactive species, namely the hydroxyl radicals. The process appears then to be highly efficient for the oxidation of the pollutants sulfasalazine and sulfapyridine. Under our experimental conditions, the process was optimized in terms of concentrations of the photocatalyst, hydrogen peroxide and pollutant concentrations and also in term of pH. For both pollutants, the analysis of the generated by-products, using HPLC/MS, shows that the degradation proceeds primarily through three and common chemical processes: i) hydroxylation ii) desulfurization and iii) scission at the azo group -N=N-. The attack of the hydroxyl radical is clearly the main species for the degradation processes. As clearly demonstrated by the TOC experiments, the combination of $W_{10}O_{32}^{4-}/H_2O_2/h\nu$ system permitted a total mineralization of the solution indicating its high efficiency for the a potential application of water depollution.

1. Introduction

Nowadays, the emergence of antibiotics in the environment and their potential hazards have attracted more and more attention [1-3]. Most antibiotics are not completely absorbed by the body, and an average of more than 50-90% of the antibiotics are excreted in the form of protoplasts or metabolites, which have been widely detected in surface water, groundwater, sewage treatment plant effluent, drinking water and soil sediments [4]. For example, antibiotics such as ofloxacin at 306 ng L^{-1}, lincomycin at 249 ng L^{-1} and spiramycin at 74 ng L^{-1} and trace amounts of amoxicillin and penicillin were detected in the Lambro and Po rivers in Italy at significant concentrations [5]. The presence of antibiotics into the environment not only has adverse effects on the ecosystem, such as the emergence of resistant pathogens and toxicity to aquatic organisms, but also can enter the human body through the enrichment of food chain, leading to a serious threat to human health such as causing vomiting or diabetes mellitus [6, 7]. The common occurrence of abusing of antibiotics is easily found especially in aquaculture field in some Asian countries like China and India. China has been one of the largest producers and users of the antibiotics in the world, approximately 162 000 tons of antibiotics were used in 2013. Aquaculture consumption accounted for about 52% of the total antibiotics [8]. Therefore, the treatment of antibiotics in the environment is particularly important.

The biological, adsorption and chemical oxidation methods, etc. were applied in treating the antibiotics present in wastewater. For example, Xiong et al. combined amino-functionalized Metal-organic framework (MOFs, MIL-53(Fe)) with multi-walled carbon nanotubes (MWCNT) to synthesize a novel adsorbent composite which was used to adsorb tetracycline hydrochloride (TCN) and chlortetracycline hydrochloride (CTC) [9]. While antibiotics are composed by various functional groups and substituents, the structure is very different, which makes the adsorption behavior on adsorbents different for distinct antibiotics and so the efficiency of the treatment will be strongly chemical structure dependent.

Advanced oxidation processes (AOPs), also known as deep oxidation technology, are characterized by the generation of reactive species (reactive oxygen species “ROS”), such as hydroxyl radicals ($HO^{\bullet}$), sulfate radicals ($SO_4^{\bullet-}$), with strong oxidizing power [10]. The organic substances which are difficult to degrade, can be oxidized into a low-toxic or non-toxic small molecule substance, and very often more readily (bio-)degradable, [4, 11-15]. Due to its green environmentally friendly sustainable properties, the photocatalytic oxidation became one of the best

promising techniques in treating organic wastewater. Many researchers develop important energy in the synthesis of new photocatalysts or the modification of already prepared photocatalyst with the aim to improve the efficiency of organic pollutants degradation.

The decatungstate anion ($W_{10}O_{32}^{4-}$) was shown to be one of the most photo-chemically active polyoxometalates, which catching the interesting of thousands of researchers over the past 30 years [16]. It is worth noting that $W_{10}O_{32}^{4-}$ absorbs in the UV with a maximum at 320 nm and its absorption spectrum presents a useful overlap with the solar emission spectrum. Illumination of $W_{10}O_{32}^{4-}$, within the range 300 - 400 nm, leads to the formation of an oxygen-to-metal charge transfer excited state $W_{10}O_{32}^{4-}$* that decays in less than 30 ps to an extremely reactive non-emissive transient, which has been referred to as wO [17]. This latter species is able to oxidize organic compounds through electron transfer or/and hydrogen abstraction owing to the presence of an electron-deficient oxygen center. In decatungstate system, the reactive species has a lifetime τ_{wO} of 65±5 ns in the case of sodium decatungstate and its formation quantum yield Φ_{wO} is 0.57 [17]. Such reaction between wO and appropriate hydrogen or/and electron donor leads to the formation of the one electron reduced form of decatungstate $W_{10}O_{32}^{5-}$ that absorbs in the visible region with a maximum at 778 nm. The reduction of molecular oxygen to superoxide anion by such species is an efficient process for the regeneration of the starting catalyst, $W_{10}O_{32}^{4-}$. In previous studies, the decatungstate ($W_{10}O_{32}^{4-}$) was used as an efficient and optimistic tool in organic synthesis, which can functionalize some organic compounds such as alkanes, alkenes, alcohols, aldehydes and sulfides in organic and aqueous media via free radical carbon-centered intermediates [18]. On the other hand, the decatungstate was also deeply studied for water depollution. Allaoui et al. studied the photodegradation of 2-mercaptobenzothiazole (MBT) and illustrated that the photodegradation rate of MBT clearly increased in the presence of decatungstate ($W_{10}O_{32}^{4-}$) by a factor of six when compared with the direct photolysis; and oxygen appeared to be the key species for catalyst regeneration [19].

In the present work, we choose the soluble sodium decatungstate ($Na_4W_{10}O_{32}$) as a photocatalyst to degrade the sulfonamides antibiotics (sulfasalazine and sulfapyridine). Moreover, and in this homogeneous system, we added hydrogen peroxide as a supplementary oxidant (with oxygen) in order to oxidize the reduced species of decatungstate ($W_{10}O_{32}^{5-}$) permitting the efficient

regeneration of the starting $W_{10}O_{32}^{4-}$. This additional process permits the formation of the highly reactive species, namely hydroxyl radicals. Our purpose was to evaluate the photodegradation of sulfasalazine (SSZ) and sulfapyridine (SPD) through the determination of kinetics, the initial rate constants and the yields of SSZ and SPD degradation. In addition, with the photoproducts identification, the mechanistic pathways involved in the degradation will be proposed with the aim to have a better insight into the SSZ and SPD degradation scheme.

2. Materials and Methods

2.1. Materials

Sulfasalazine (SSZ) (99.8%), Sulfapyridine (SPD) (≥99%), sodium tungstate ($Na_2WO_4{\cdot}2H_2O$), sodium chloride (NaCl), hydrochloric acid (HCl), hydroperoxide (H_2O_2), perchloric acid ($HClO_4$), and sodium hydroxide (NaOH) were purchased from Sigma Aldrich and used as received. Water was purified using a reverse osmosis RIOS 5 and Synergy (Millipore) device (resistivity 18 MΩ·cm, DOC < 0.1 $mg{\cdot}L^{-1}$).

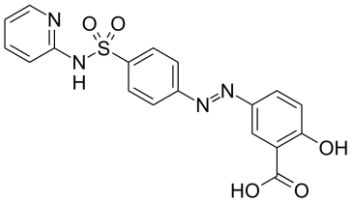

SSZ

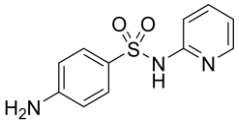

SPD

2.2. Preparation and characterization of sodium decatungstate

The preparation of sodium decatungstate refers to the previous studies available [20]. The boiling sodium tungstate solution (50 g of Na_2WO_4, $2H_2O$ dissolved in 300 mL of ultrapure water) was mixed with 1.0 M boiling hydrochloric acid (300 mL) in a beaker, refluxed for 20 seconds to form a green solution. It was followed by adding 150 g of solid sodium chloride, stirring until the solution has been re-boiled and keeping for 20 seconds, then rapidly putting into the ice-water bath. This suspension solution was maintained in a freezer (-18°C) overnight. The next day, this suspension solution of NaCl and crude $Na_4W_{10}O_{32}$ was filtered and the solid was dissolved into 150 mL of acetonitrile solution. The acetonitrile solution was refluxed for 5 min at 79°C and filtered to remove the insoluble NaCl after cooling at ambient temperature. The acetonitrile solution was gently

evaporated in hot-water bath (79°C) to obtain the yellow-green catalyst.

The UV-Vis absorption spectra were obtained using a Varian Cary 300 UV-visible spectrophotometer. The infrared absorption spectra were obtained by Fourier infrared absorption spectrometer, operated by potassium bromide pressed-disk technique (98% KBr).

2.3 Irradiation experiments and photoreactor

Irradiation experiments (365 nm) were carried out in a stainless-steel cylindrical reactor. Six high pressure mercury lamps (Philips HPW, 15W, emission centered at 365 nm) was located evenly on the edge of the cylinder with a fan placed on the bottom of the cylinder to cool the irradiation system. The reactor, a Pyrex tube (2 cm diameter), was placed at the center of the cylinder (**Figure S1**).

The degradation of SSZ and SPD was performed in a batch experiment. The 5.0×10^{-5} M solution of SSZ and SPD was prepared and 10.0 mg soluble decatungstate was added into the 100 mL of SSZ or SPD solution, the concentration of decatungstate was then evaluated to 4.0×10^{-5} M. Hydrogen peroxide was added using a concentrated solution, and so with negligible volume, prior to irradiation using the photo-reactor system. The pH of solution was adjusted to 4.0 $\pm$ 0.05 using perchloric acid and sodium hydroxide (0.1 M). Aliquots were taken at different interval times of 0, 2, 5, 10, 15, 20, 25 min at ambient temperature.

The effect of initial pH was studied at 23 °C using a similar procedure, 10 mg decatungstate (4.0×10^{-5} M) were mixed with 100 mL 5.0×10^{-5} M solution of SSZ or SPD at different initial pH of 3, 4, 5 and 6. The solution pHs were adjusted by adding small negligible volume of perchloric acid and/or sodium hydroxide (0.1 M).

The effect of the concentration of H_2O_2 (from 10^{-5} to 10^{-2} M), SSZ and SPD (5.0×10^{-6}, 10^{-5}, 2.0×10^{-5}, 5.0×10^{-5} and 1.0×10^{-4} M) and decatungstate (2.0×10^{-5}, 4.0×10^{-5}, 7.0×10^{-5}, 1.0×10^{-4} and 2.0×10^{-4} M) were also investigated.

2.4 HPLC Analysis

The concentrations of SSZ and SPD were evaluated by HPLC (Shimadzu NEXERA XR HPL) equipped with a photodiode array detector and an auto sampler. The column was a Macherey Nagel EC 150/2 NUCLEODUR C18ec (150 mm × 2 mm, 2 μm particle size)

The analysis of SSZ was performed using methanol (MeOH, solvent B) as mobile phase and

water with 0.5 % phosphoric acid (solvent A) at a flow rate of 0.20 mL min^{-1}. The elution was performed using the following gradient: 40 % of B for 5min, linear increase of B to 95 % in 15 min, 95 % of B for 5 min and decrease of B to 40 % in 0.1 min. For SPD, the analyses were performed using acetonitrile (ACN, solvent C) as mobile phase and water with 0.5 % of phosphoric acid at a flow rate of 0.40 mL min^{-1}. The elution was performed using the following gradient: 5 % of C for 2.5 min, linear increase of C to 40 % in 4.5 min, then increase of C to 95 % in 1.5 min, 95 % of C for 1 min and decrease of C to 5 % in 0.5 min.

The identification of degradation products was performed using high resolution mass spectrometry (HRMS) constituted of an Orbitrap Q-Exactive (Thermoscientific) coupled to an ultra-high performance liquid chromatography (UHPLC) instrument Ultimate 3000 RSLC (Thermoscientific). Analyses were carried out in both negative and positive electrospray modes (ESI^+ and ESI^-). SSZ, SPD and the degradation products were separated using the same elution gradient as previously indicated. The column was a Kinetec EVO C18 Phenomenex (100 mm × 2.1 mm, particle size of 1.7 μm) and the flow rate was set at 0.45 $mL \cdot min^{-1}$.

2.5 TOC Analysis

The concentration of the total organic carbon (TOC) in the aqueous solution was followed on a Shimadzu TOC 5050A analyzer. The TOC value was the average of three individual injections.

3. Results

3.1. Characterization and photochemistry behavior of the photocatalyst

The UV-visible spectrum of the synthesized photocatalyst decatungstate, $W_{10}O_{32}^{4-}$ (**W**), is given in **Figure 1**. It shows an absorption band with a defined maximum at 321 nm and a molar absorption coefficient of 12365 M^{-1} cm^{-1} in perfect agreement with the published literature data [20]. The UV absorption extends up to 400 nm indicating an important and interesting overlap with the emission spectrum of solar light. In addition to the UV visible spectrum, the characterization of the decatungstate was also performed by employing the Fourier transformed IR. In **Figure S2**, the strong broad band centered at around 3500 cm^{-1} and the peak at around 1600 cm^{-1} are attributed to the O–H

stretching vibrations and to the bending modes of water molecules. This implied that the hydrophilicity of the substrate will improve the photocatalysis acitivity as suggested by H-Y. He [21, 22]. The main vibration bands of decatungstate ($W_{10}O_{32}^{4-}$) are observed at 1006 cm^{-1} corresponding to the stretching vibration of the W=O bond, and at 962, 915, 796, 667, 586, 431 cm^{-1} due to the deformation of W-O-W bonds [17, 23, 24]. Moreover, and as largely reported in the literature [16, 25, 26], the excitation of the mixture decatungstate and methanol (used as a sacrificial agent since it acts as an electron or/and hydrogen donor) permits in deoxygenated conditions the formation of a blue component that presents two well defined bands with maximums at 360 and 780 nm **(Figure S3)** with roughly similar molar absorption coefficients (6.7-6.9 × 10^3 M^{-1} cm^{-1} at 360 nm and 9.5-11 × 10^3 M^{-1} cm^{-1} at 780 nm). Such absorptions are owing to the formation of the reduced species of decatungstate, namely $W_{10}O_{32}^{5-}$ that disappears rapidly by bubbling oxygen through an electron transfer process leading to the formation of superoxide anion radical $O_2^{\bullet-}$ with the simultaneous regeneration of the starting photocatalyst decatungstate [27] (**Scheme 1**). Such interesting behavior was used within the present work to enhance the ability of the photocatalyst to decontaminate polluted waters by producing reactive oxygen species (ROS) that are highly oxidant such as hydroxyl radical. The formation of this latter species was reached by introducing hydrogen peroxide as a sacrificial reactant.

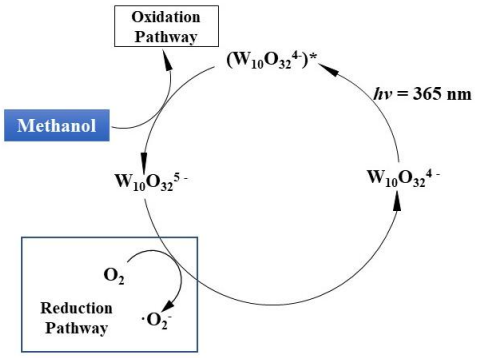

Scheme 1: Photocatalytic cycle of decatungstate upon UV excitation in the presence of methanol showing oxidation and reduction processes.

The efficiency of the photocatalytic cycle was studied and optimized by studying sulfonamides antibiotics sulfasalazine (SSZ) and sulfapyridine (SPD) degradations.

3.2. Degradation of SSZ and SPD by decatungstate, H_2O_2 or decatungstate/H_2O_2 systems under UVA irradiation

In order to evaluate the efficiency of the decatungstate photocatalysis process, irradiations were performed under UVA (365 nm) for different aerated solutions in the presence of SSZ in various conditions (SSZ alone, SSZ + H_2O_2, SSZ + W and SSZ + H_2O_2 + W). As clearly shown in **Figure 2A,** no degradation was noted when SSZ was alone in aqueous solution, despite its significant absorption at the excitation wavelength. This indicates the relative photochemical stability of SSZ under our experimental conditions. However, in the presence of hydrogen peroxide, a negligible degradation was observed representing 2% within 120 minutes of irradiation. In the presence of decatungstate, the conversion percentage of SSZ reached 16% demonstrating the oxidation ability of the photocatalyst decatungstate through an oxidation process (electron transfer) as shown in **Scheme 1.** The initial rate of SSZ disappearance was estimated to 1.2×10^{-7} M min^{-1}. By addition of hydrogen peroxide in the previous system, the conversion percentage increased significantly in agreement with the fact that hydrogen peroxide interacts in the photocatalytic cycle and presents a positive and beneficial effect when it is used simultaneously with decatungstate. In this latter system, the degradation of SSZ reaches 28% after 120 minutes irradiation time with an initial rate of 1.6×10^{-7} M

min^{-1}. The benefit of hydrogen peroxide in the photocatalysis process is then effective and it was deeply studied and optimized within the present work. Similar experiments were performed with SPD showing a more pronounced degradation. This is owing to the fact that SPD does not absorb at the excitation wavelength, in contrary to SSZ, and thus no competition of the absorbed light intensity is involved (**Figure 2B**). The initial rate of SPD degradation was estimated to 4.3×10^{-7} M min^{-1} and 7.0×10^{-7} M min^{-1} in the presence of decatungstate and decatungstate/H_2O_2 respectively.

The involvement of hydrogen peroxide in the photocatalytic system was also studied by analyzing its reactivity with the reduced species of decatungstate, namely $W_{10}O_{32}^{5-}$. As shown in **Scheme 1**, the latter species was selectively formed by irradiation of **decatungstate** (40 μM) in the presence of 1 % of methanol in deaerated solution. $W_{10}O_{32}^{5-}$ immediately disappears when hydrogen peroxide is added to the solution with the regeneration of the $W_{10}O_{32}^{4-}$. It is then clear that H_2O_2 is efficiently reduced by $W_{10}O_{32}^{5-}$ owing, very likely, to the following Fenton like process (**Equation 1**).

$$W_{10}O_{32}^{5-} + H_2O_2 \longrightarrow W_{10}O_{32}^{4-} + {}^{\bullet}OH + {}^{-}OH$$

Equation 1: Fenton like reaction between $W_{10}O_{32}^{5-}$ and H_2O_2.

The effective formation of hydroxyl radical as a reactive oxygen species (**ROS**) was demonstrated by employing a probe such as terephthalic acid. As largely reported in the literature, the reactivity of this non fluorescent substrate with hydroxyl radical leads to the formation of a highly fluorescent hydroxyterephthalic acid [28]. As clearly shown in **Figure 3,** the excitation of aerated aqueous solution of decatungstate (W) in the presence of terephthalic acid (TA) and hydrogen peroxide (H_2O_2) at pH = 4.0 leads to a rapid and efficient formation of hydroxyterephthalic acid (TAOH) from the early stages of the irradiation. This demonstrates the involvement of an additional pathway for the formation of the reactive oxygen species, namely the hydroxyl radical. The absence of the blue color following irradiation is a clear evidence for involvement of the reduced species of decatungstate ($W_{10}O_{32}^{5-}$) for the formation of this **ROS** species. The smaller amount of hydroxyl radical in the absence of hydrogen peroxide could be due to the disproportionation process of hydroperoxide radical and/or superoxide anion radical ($HO_2^{\bullet}/O_2^{\bullet-}$) to form H_2O_2 [29]. It is than clear from these results that the amount of hydroxyl radical mainly originates from the reactivity of

$W_{10}O_{32}^{5-}$ and hydrogen peroxide permitting the implication of a supplementary pathway for the degradation of the pollutants: first through the oxidation by the excited state of decatungstate via an electron transfer or/and hydrogen transfer processes and then through the oxidation by the hydroxyl radical generated via the Fenton like process **(Scheme 2).** It should be pointed out that the latter reaction is in competition with the reactivity of $W_{10}O_{32}^{5-}$ with oxygen.

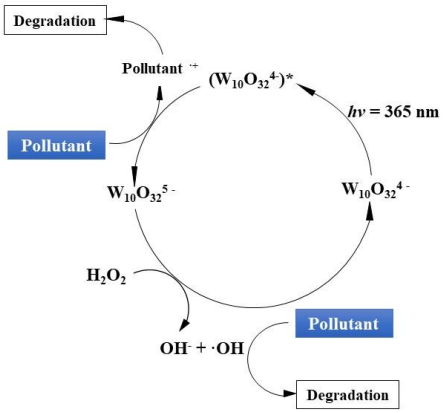

Scheme 2: Photocatalytic cycle of decatungstate in the presence of H_2O_2 showing the two ways for the organic pollutant degradation.

In the following parts of the paper, the optimization of the experimental conditions was studied by analyzing the effect of various parameters such as: concentrations of decatungstate; hydrogen peroxide and organic pollutant and the initial pH of the solution. These parameters represent fundamental parameters for the photocatalysis to be effective since i) decatungstate is the absorbing species and thus its optimum concentration will insure high concentration of the excited state without the negative inner filter effect ii) hydrogen peroxide efficiently contributes in the system to the formation of hydroxyl radicals. The latter species react simultaneously with the pollutant and hydrogen peroxide via competitive reactions and iii) the stability of the photocatalyst depends on the solution pH.

3.3. Effect of different amount of decatungstate

In order to study the effect of decatungstate concentration on the removal of the pollutants SSZ and SPD, the experiments were performed at pH= 4.0. As clearly shown in **Figure 4A and 4B,** the degradation rates of SSZ and SPD increase by increasing the concentration of the photocatalyst decatungstate. This effect is without any doubt due to the increase of the light absorption by

decatungstate at higher concentration. However, under our experimental conditions the degradation rate rapidly levelled off when decatungstate concentration reaches 50 µM, as shown in **Figure 4C.** This is more probably owing to the inner filter effect. Thus, the concentration close to 40 µM was chosen as the optimal concentration of the photocatalyst for the following experiments.

3.4. Effect of different concentrations of H_2O_2

Table 1 gathers the initial degradation rate obtained for both pollutants by excitation of decatungstate (40 µM) in the presence of various hydrogen peroxide concentrations. In the absence of H_2O_2 and at lower concentration of H_2O_2 (1 mM), the disappearance initial rate is found roughly 4 times higher for SPD than for SSZ due to the absorption of light by SSZ. At higher concentrations of H_2O_2 (10 to 100 mM), the disappearance initial rate of SPD is always higher than that of SSZ but by a factor of about 1.5. In addition to the electron transfer between SSZ or SPD and $W_{10}O_{32}^{4-}$ excited state, a second pathway is involved when hydrogen peroxide is added to the system via the production of hydroxyl radicals as demonstrated above. As clearly shown in **Table 1**, this reaction is effective despite the presence of dissolved molecular oxygen at a concentration of 2.6×10^{-4} M [30, 31]. Moreover, the initial disappearance rate increases when hydrogen peroxide concentration increases. One should also note, that under our experimental conditions and at high concentrations, the direct light absorption by hydrogen peroxide also participate in the generation of hydroxyl radical and thus to the degradation of the pollutant through the homolytic scission of O-O bond [32, 33]. It should be noted that at high concentration of hydrogen peroxide, the consumption of hydroxyl radical could be observed by H_2O_2 itself which is detrimental under our experimental conditions [34, 35].

3.5. Effect of different SSZ and SPD concentrations

With the aim to use the photocatalyst decatungstate for various pollutants that have different chemical structures and also different light absorption profiles, we undertook the effect of the concentration of both pollutants, SSZ and SPD, on the efficiency of the photocatalytic process. We can note that SPD does not absorb at the excitation wavelengths, namely at 365 nm, while SSZ shows significant absorbance with a molar absorption coefficient $\varepsilon_{365\ nm} = 21850.4\ M^{-1}\ cm^{-1}$. The

experiments were performed by using decatungstate at the concentration of 40.0 µM in the presence of H_2O_2 10 mM with various concentrations of the pollutants within the range 5.0 to 100 µM at pH = 4.0. As shown in **Figure 5**, the initial disappearance rate of SPD increased by increasing its initial concentration. This clearly shows that under our experimental conditions, hydroxyl radical is involved in the oxidation of SPD but it is also trapped by hydrogen peroxide as largely reported in the literature with a rate constant of 3.0×10^{7} M^{-1} s^{-1} [34, 35]. Such reaction is detrimental since it participates to the decrease of the stationary concentration of the reactive species: hydroxyl radical. So, the use of relatively high concentrations of SPD will be in favor of its degradation.

In the case of SSZ, the initial rate first increases within the concentration range 5.0 to 20.0 µM and then decreases at higher concentrations. Such decrease of the initial rate is mainly owing to the competition in the absorption of light intensity involving the photocatalyst decatungstate and SSZ. Such effect is detrimental to the photocatalysis effect and leads to the decrease of the concentration/formation of reactive excited state of decatungstate, namely, $W_{10}O_{32}^{4-}$*.

3.6. Effect of different initial pH

The initial pH of the solution is a crucial parameter for the photocatalysis processes owing to the stability of decatungstate and/or the various forms of the pollutants when a protonation-deprotonation process is present (**Figure S4**). Thus, we studied the optimum pH under our experimental conditions. For both substrates, SSZ and SPD at a concentration of 50.0 µM, the excitation of decatungstate (40 µM) at 365 nm in the presence of 1.0 mM H_2O_2 permitted the degradation of the pollutants with a rate that decreases when the pH of the solution increases. The initial rates of SSZ were estimated to 2.1×10^{-7} M min^{-1} and 1.1×10^{-7} M min^{-1} at pH = 3.0 and 6.0 respectively and the initial rates of SPD were estimated to 7.4×10^{-7} M min^{-1} and 5.5×10^{-7} M min^{-1} at pH = 3.0 and 6.0 respectively. This effect is more likely due to the fact that decatungstate is relatively instable at high pH values as largely reported in the literature [29, 36].

3.7. Elucidation of the initial products and degradation pathways for the pollutant disappearance

The elucidation of the generated byproducts was performed by employing HPLC/MS technique.

The results are gathered in **Table 2** for both substrates: SSZ and SPD. They were obtained for irradiated samples that show roughly 30% conversion corresponding under our experimental conditions to 120 min of irradiation time. The suggested structures were based on the elemental compositions that were obtained from the obtained accurate masses. Some of them are clearly primary products while others originate from secondary reactions.

The analysis of the chemical structures of the products leads us to the conclusion that in the early stages of the irradiation mainly three and common chemical processes are involved for both pollutants: i) hydroxylation ii) desulfurization and iii) scission at the azo group -N=N-.

The hydroxylation process is a clear evidence of the reactivity of the hydroxyl radical with the used pollutants via an electron transfer process with the aromatic groups as largely reported in the literature [37-39] leading finally to the addition of the hydroxyl group to the substrate (**scheme 3).**

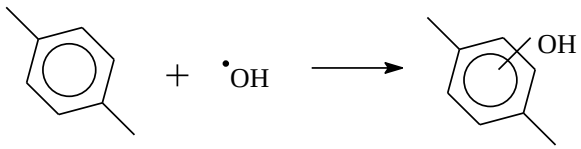

Scheme 3: Process of the reactivity of the hydroxyl radical with the benzene ring via an electron transfer process

The desulfurization reaction is a reaction that is more likely triggered by the attack of the hydroxyl radical on the adjacent amine group via an electron or/and a hydrogen abstraction process followed by an intramolecular rearrangement as shown in the following **scheme 4 [40]**.

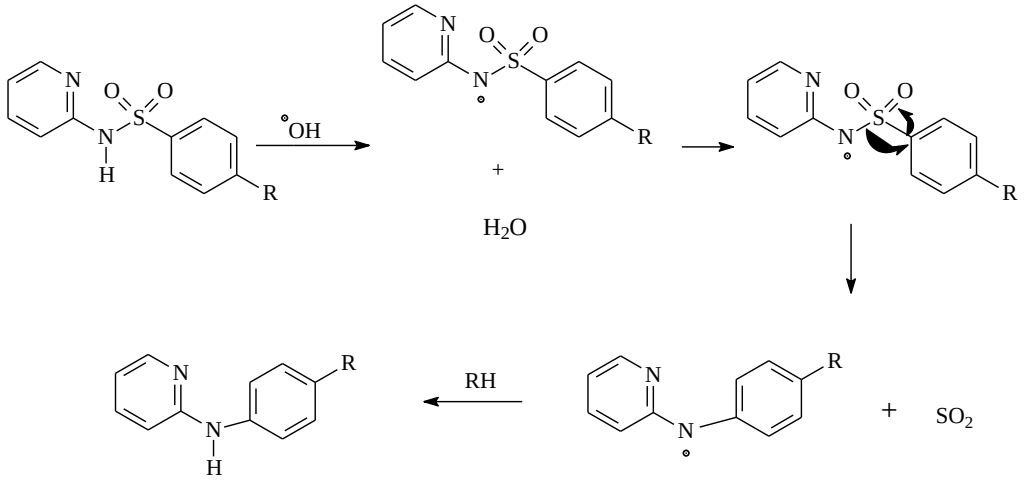

Scheme 4: The process of the desulfurization via an electron or/and a hydrogen abstraction process.

The third process is a scission at the azo group -N=N- that is more likely triggered by the attack of the hydroxyl radical on the nitrogen sites leading to the formation of the two amine products as shown in the following **scheme 5 [41]**

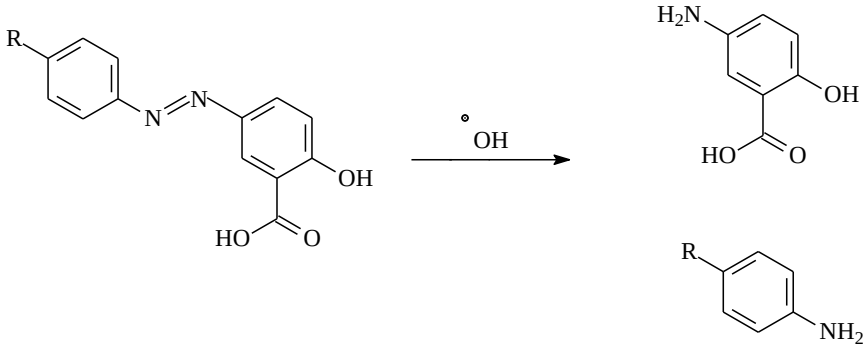

Scheme 5: Process of the azo group -N=N- scission via an attack of hydroxyl radical.

The photocatalytic process; involving decatungstate and H_2O_2 is given in **Scheme 6**. $W_{10}O_{32}^{4-}$ could be excited upon UVA (365 nm) irradiation to form the excited state $W_{10}O_{32}^{4-*}$ which leads, via an electron transfer process with the pollutant, to the formation of the reduced form of decatungstate namely $W_{10}O_{32}^{5-}$ and the radical cation of the pollutant. This process provides one of the degradation pathways. The regeneration of the photocatalyst can operate in the presence of H_2O_2 and oxygen, following the formation of the hydroxyl radicals and superoxide anion radicals respectively. The former free radical is highly and efficiently involved in the oxidation of SPD and SSZ. And this represents the second pathway of organic pollutant degradation.

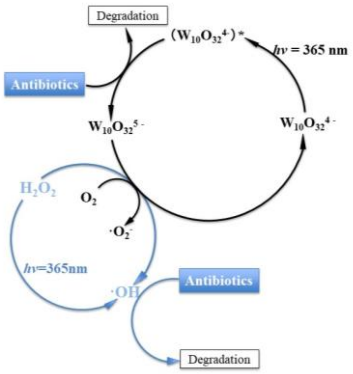

Scheme 6: Photocatalytic cycle of decatungstate/H_2O_2 system showing the two ways for the

degradation of the organic pollutant and the production of hydroxyl radicals via Fenton like reaction between $W_{10}O_{32}^{5-}$ and H_2O_2.

3.8. Total organic carbon analysis

In order to confirm the efficient degradation of the pollutants and also of their metabolites up to the mineralization of the solution, we followed the total organic carbon (TOC) under light excitation. We followed the evolution of TOC in a solution of SPD or/and SSZ under similar conditions ([W] = 40.0 μM, $[H_2O_2]$ = 10.0 mM, pH = 4.0). In this case, after 24 h of irradiation, 90% of the initial organic carbon (SSZ alone) has been transformed into CO_2 (**Fig. 6**). After 48h of irradiation, 75% of the initial organic carbon (SPD alone, SPD and SSZ) has been converted into CO_2 (**Fig. 6**). Such observations confirm that the decatungstate/H_2O_2 system could be used in order to completely achieve the removal of SPD or/and SSZ and their byproducts from water. Moreover they suggest that decatungstate/H_2O_2 system could be applied to treat multiple pollutants in water under the optimized experimental conditions.

4. Conclusion

The combination of $W_{10}O_{32}^{4-}/H_2O_2/h\nu$ at pH=4.0 permitted an efficient degradation of the pollutants sulfasalazine and sulfapyridine. The process involves two ways of reaction for the oxidation of the organic compounds i) an electron transfer reaction with the excited state of decatungstate and ii) also the hydroxyl radical reactivity. $HO^{\bullet}$ is formed from the Fenton like reaction with the reduced species of decatungstate, $W_{10}O_{32}^{5-}$ and H_2O_2. The latter process represents under our experimental conditions the main process for the disappearance of the pollutants and it is also a way for the regeneration of starting catalyst, decatungstate. The main primary reactions were found to be hydroxylation, desulfurization and scission at the azo group -N=N- moiety. For prolonged irradiations, the mineralization of the solution was observed which highlights the point that the conjunction of $W_{10}O_{32}^{4-}/H_2O_2$ and light represent an interesting AOP's system for water depollution. Indeed, the two possible pathways for the oxidation of organic compounds in this system are important asset for treating polluted waters leading us to the conclusion that this system could be considered in the future as a promising process for the decontamination of water. As a

perspective of this work, the immobilization of the photocatalyst decatungstate on solid supports will be a goal in order to recycle the photocatalyst after treatment.

Acknowledgements

Peng CHENG thanks the Chinese scholarship council for its financial support and thanks professor Marcello Brigante, engineer Guillaume Voyard and PhD student Yara Arbid for their help in some of the experiments.

References

[1] R. Laxminarayan, A. Duse, C. Wattal, A.K. Zaidi, H.F. Wertheim, N. Sumpradit, E. Vlieghe, G.L. Hara, I.M. Gould, H. Goossens, Antibiotic resistance—the need for global solutions, The Lancet infectious diseases, 13 (2013) 1057-1098.

[2] C. Ding, J. He, Effect of antibiotics in the environment on microbial populations, Applied microbiology and biotechnology, 87 (2010) 925-941.

[3] M. Qiao, G.-G. Ying, A.C. Singer, Y.-G. Zhu, Review of antibiotic resistance in China and its environment, Environment international, 110 (2018) 160-172.

[4] Lucilaine Valéria de Souza Santos, Alexandre Moreira Meireles, Liséte Celina Lange, Degradation of antibiotics norfloxacin by Fenton, UV and UV/H2O2, Journal of environmental management, 154 (2015) 8-12.

[5] D. Calamari, E. Zuccato, S. Castiglioni, R. Bagnati, R. Fanelli, Strategic survey of therapeutic drugs in the rivers Po and Lambroin northern Italy, Environ. Sci. Technol., 37 (7) (2003) 1241–1248.

[6] B.A. Cunha, Antibiotic side effects, Medical Clinics of North America, 85 (2001) 149-185.

[7] A. Sola, Abuse of antibiotics in perinatology: negative impact for health and the economy, NeoReviews, 21 (2020) e559-e570.

[8] Q.-Q. Zhang, G.-G. Ying, C.-G. Pan, Y.-S. Liu, J.-L. Zhao, Comprehensive Evaluation of Antibiotics Emission and Fate in the River Basins of China: Source Analysis, Multimedia Modeling, and Linkage to Bacterial Resistance, Environmental Science & Technology, 49 (2015) 6772-6782.

[9] W. Xiong, Z. Zeng, X. Li, G. Zeng, R. Xiao, Z. Yang, Y. Zhou, C. Zhang, M. Cheng, L. Hu, Multi-walled carbon nanotube/amino-functionalized MIL-53 (Fe) composites: remarkable adsorptive removal of antibiotics from aqueous solutions, Chemosphere, 210 (2018) 1061-1069.

[10] T. Oppenländer, Photochemical purification of water and air: advanced oxidation processes (AOPs)-principles, reaction mechanisms, reactor concepts, John Wiley & Sons, 2007.

[11] L. Hu, P. Wang, T. Shen, Q. Wang, X. Wang, P. Xu, Q. Zheng, G. Zhang, The application of microwaves in sulfate radical-based advanced oxidation processes for environmental remediation: A review, Science of The Total Environment, (2020) 137831.

[12] J. Deng, Y. Shao, N. Gao, Y. Deng, S. Zhou, X. Hu, Thermally activated persulfate (TAP) oxidation of antiepileptic drug carbamazepine in water, Chemical Engineering Journal, 228 (2013) 765-771.

[13] F. Sopaj, N. Oturan, J. Pinson, F.I. Podvorica, M.A. Oturan, Effect of cathode material on electro-Fenton process efficiency for electrocatalytic mineralization of the antibiotic sulfamethazine,

Chemical Engineering Journal, 384 (2020) 123249.
[14] L. Hou, H. Zhang, X. Xue, Ultrasound enhanced heterogeneous activation of peroxydisulfate by magnetite catalyst for the degradation of tetracycline in water, Separation and Purification Technology, 84 (2012) 147-152.
[15] M. Xing, W. Xu, C. Dong, Y. Bai, J. Zeng, Y. Zhou, J. Zhang, Y. Yin, Metal sulfides as excellent co-catalysts for H2O2 decomposition in advanced oxidation processes, Chem, 4 (2018) 1359-1372.
[16] C. Tanielian, Decatungstate photocatalysis, Coordination Chemistry Reviews, 178-180 (1998) 1165-1181.
[17] I. Texier, J.A. Delaire, C. Giannotti, Reactivity of the charge transfer excited state of sodium decatungstate at the nanosecond time scale, Physical Chemistry Chemical Physics, 2 (2000) 1205-1212.
[18] M.D. Tzirakis, I.N. Lykakis, M. Orfanopoulos, Decatungstate as an efficient photocatalyst in organic chemistry, Chemical Society Reviews, 38 (2009) 2609-2621.
[19] A. Allaoui, M.A. Malouki, P. Wong-Wah-Chung, Homogeneous photodegradation study of 2-mercaptobenzothiazole photocatalysed by sodium decatungstate salts: Kinetics and mechanistic pathways, Journal of Photochemistry and Photobiology A: Chemistry, 212 (2010) 153-160.
[20] D.C. Duncan, T.L. Netzel, C.L. Hill, Early-Time Dynamics and Reactivity of Polyoxometalate Excited States. Identification of a Short-Lived LMCT Excited State and a Reactive Long-Lived Charge-Transfer Intermediate following Picosecond Flash Excitation of [W10O32]4- in Acetonitrile, Inorganic Chemistry, 34 (1995) 4640-4646.
[21] H.-Y. He, J. Lu, Highly photocatalytic activities of magnetically separable reduced graphene oxide-CoFe2O4 hybrid nanostructures in dye photodegradation, Separation and Purification Technology, 172 (2017) 374-381.
[22] H.-Y. He, Z. He, Q. Shen, Efficient hydrogen evolution catalytic activity of graphene/metallic MoS2 nanosheet heterostructures synthesized by a one-step hydrothermal process, International Journal of Hydrogen Energy, 43 (2018) 21835-21843.
[23] M. Bonchio, M. Carraro, M. Gardan, G. Scorrano, E. Drioli, E. Fontananova, Hybrid photocatalytic membranes embedding decatungstate for heterogeneous photooxygenation, Topics in Catalysis, 40 (2006) 133-140.
[24] Y. Guo, C. Hu, X. Wang, Y. Wang, E. Wang, Y. Zou, H. Ding, S. Feng, Microporous Decatungstates: Synthesis and Photochemical Behavior, Chemistry of Materials, 13 (2001) 4058-4064.
[25] Y. Nosaka, T. Takei, N. Fujii, Photoinduced reduction of W10O324− by organic compounds in aqueous solution, Journal of Photochemistry and Photobiology A: Chemistry, 92 (1995) 173-179.
[26] C. Tanielian, R. Seghrouchni, C. Schweitzer, Decatungstate photocatalyzed electron-transfer reactions of alkenes. Interception of the geminate radical ion pair by oxygen, The Journal of Physical Chemistry A, 107 (2003) 1102-1111.
[27] S. Rafqah, P.W.-W. Chung, C. Forano, M. Sarakha, Photocatalytic degradation of metsulfuron methyl in aqueous solution by decatungstate anions, Journal of Photochemistry and Photobiology A: Chemistry, 199 (2008) 297-302.
[28] T. Charbouillot, M. Brigante, G. Mailhot, P.R. Maddigapu, C. Minero, D. Vione, Performance and selectivity of the terephthalic acid probe for OH as a function of temperature, pH and composition of atmospherically relevant aqueous media, Journal of Photochemistry and Photobiology A: Chemistry, 222 (2011) 70-76.

[29] B.H. Bielski, Reevaluation of the spectral and kinetic properties of HO2 and O2- free radicals, Photochemistry and Photobiology, 28 (1978) 645-649.
[30] L. Wu, X. Zhang, H. Ju, Amperometric glucose sensor based on catalytic reduction of dissolved oxygen at soluble carbon nanofiber, Biosensors and Bioelectronics, 23 (2007) 479-484.
[31] H. Ju, C. Shen, Electrocatalytic reduction and determination of dissolved oxygen at a poly (nile blue) modified electrode, Electroanalysis: An International Journal Devoted to Fundamental and Practical Aspects of Electroanalysis, 13 (2001) 789-793.
[32] Y.-S. Shen, Y. Ku, K.-C. Lee, The effect of light absorbance on the decomposition of chlorophenols by ultraviolet radiation and UV/H2O2 processes, Water research, 29 (1995) 907-914.
[33] G.S. Wang, C.H. Liao, H.W. Chen, H.C. Yang, Characteristics of Natural Organic Matter Degradation in Water by UV/H2O2 Treatment, Environmental Technology, 27 (2006) 277-287.
[34] H. Christensen, K. Sehested, H. Corfitzen, Reactions of hydroxyl radicals with hydrogen peroxide at ambient and elevated temperatures, The Journal of Physical Chemistry, 86 (1982) 1588-1590.
[35] M. Alam, M. Kelm, B. Rao, E. Janata, Reaction of H with H2O2 as observed by optical absorption of perhydroxyl radicals or aliphatic alcohol radicals and of OH with H2O2. A pulse radiolysis study, Radiation Physics and Chemistry, 71 (2004) 1087-1093.
[36] E. Papaconstantinou, A. Hiskia, A. Troupis, Photocatalytic processes with tungsten oxygen anion clusters, Frontiers in Bioscience, 8 (2003) s813-825.
[37] A. Broo, S. Larsson, Electron transfer in azurin and the role of aromatic side groups of the protein, The Journal of Physical Chemistry, 95 (1991) 4925-4928.
[38] J. Howell, J. Goncalves, C. Amatore, L. Klasinc, R. Wightman, J. Kochi, Electron transfer from aromatic hydrocarbons and their. pi.-complexes with metals. Comparison of the standard oxidation potentials and vertical ionization potentials, Journal of the American Chemical Society, 106 (1984) 3968-3976.
[39] B. Krimmel, F. Swoboda, S. Solar, G. Reznicek, OH-radical induced degradation of hydroxybenzoic-and hydroxycinnamic acids and formation of aromatic products—a gamma radiolysis study, Radiation Physics and Chemistry, 79 (2010) 1247-1254.
[40] Y.-q. Zhang, X.-f. Xie, W.-l. Huang, S.-b. Huang, Degradation of aniline by Fe 2+-activated persulfate oxidation at ambient temperature, Journal of Central South University, 20 (2013) 1010-1014.
[41] A. Rehorek, M. Tauber, G. Gübitz, Application of power ultrasound for azo dye degradation, Ultrasonics Sonochemistry, 11 (2004) 177-182.

Figure captions:

Figure 1: Emission spectrum of lamps used in the reactor and UV-visible absorption spectra of SSZ, SPD and decatungstate (W)

Figure 2: Degradation kinetics of (A) SSZ and (B) SPD in the different systems. [SSZ] = [SPD] = 50 µM; [H_2O_2] = 1 mM; [W] = 40 µM; pH = 4.0

Figure 3: Formation of Hydroxyterephthalic acid by excitation of decatungstate (40 µM) at 365 nm in the presence of hydrogen peroxide (1 Mm) and terephthalic acid (50 µM) as a function of irradiation time at pH = 4.0

Figure 4: Effect of decatungstate concentration on SSZ (A) and SPD (B) removal in the presence of hydrogen peroxide. [SSZ] = [SPD] = 50 µM; [H_2O_2] = 10 mM, pH = 4.0

Figure 5: Initial degradation rates of SSZ and SPD as a function of their initial concentrations. [H_2O_2] = 10 mM; [W] = 40 µM; pH = 4.0

Figure 6: Evolution of TOC in a SSZ or/and SPD solution in decatungstate/H_2O_2 system. [H_2O_2] = 10 mM; [W] = 40 µM; pH = 4.0

Figure 1

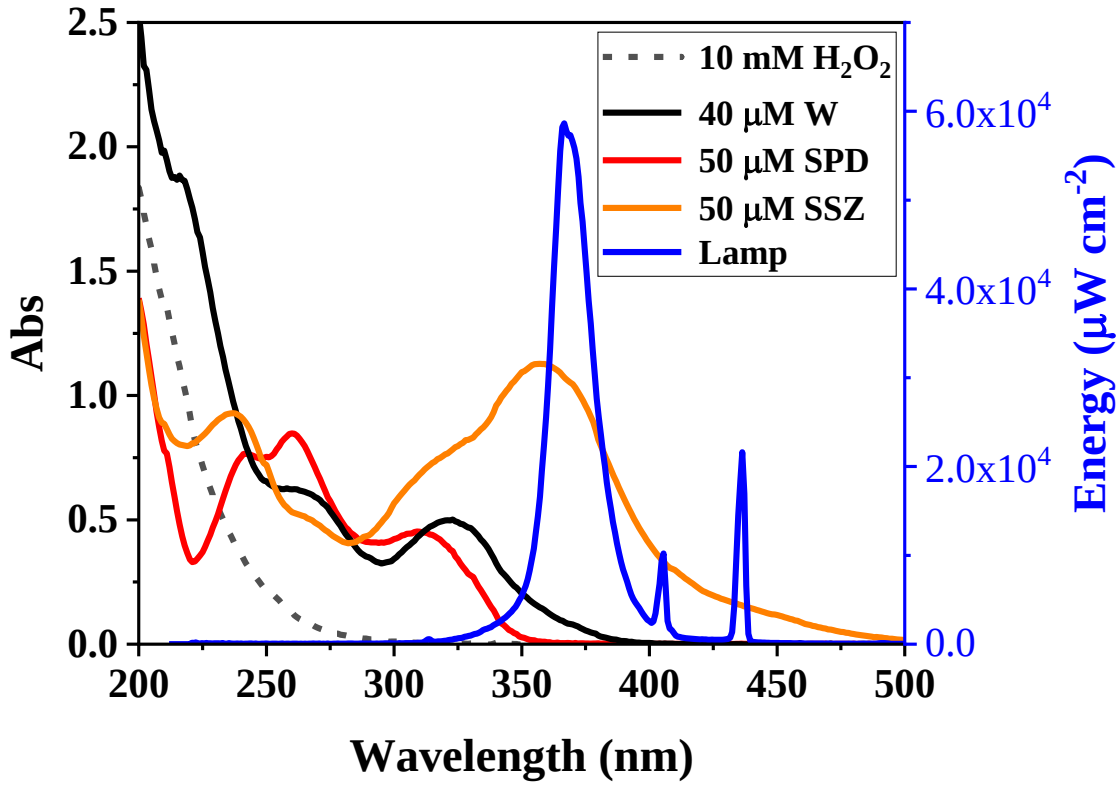
10 mM H2O2
40 μM W
50 μM SPD
50 μM SSZ
Lamp
Abs
Energy (μW cm-2)
Wavelength (nm)
2.5
2.0
1.5
1.0
0.5
0.0
200
250
300
350
400
450
500
6.0x10^4
4.0x10^4
2.0x10^4
0.0

Figure 2

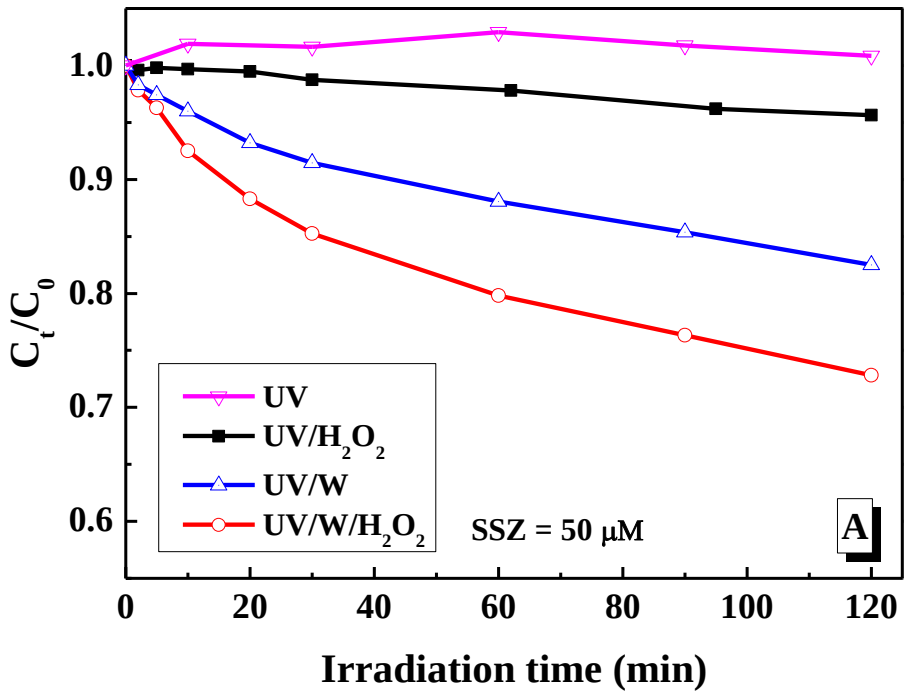
1.0
0.9
0.8
0.7
0.6
C_t/C_0
UV
UV/H_2O_2
UV/W
$UV/W/H_2O_2$
SSZ = 50 μM
A
0
20
40
60
80
100
120
Irradiation time (min)

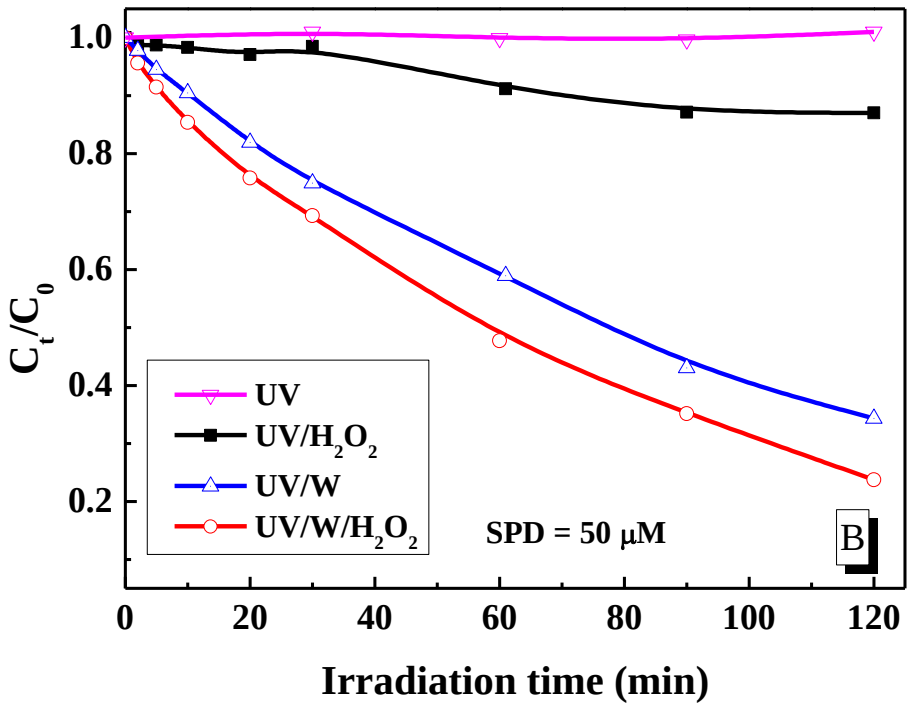
1.0
0.8
0.6
0.4
0.2
C_t/C_0
UV
UV/H_2O_2
UV/W
$UV/W/H_2O_2$
SPD = 50 μM
B
0
20
40
60
80
100
120
Irradiation time (min)

Figure 3:

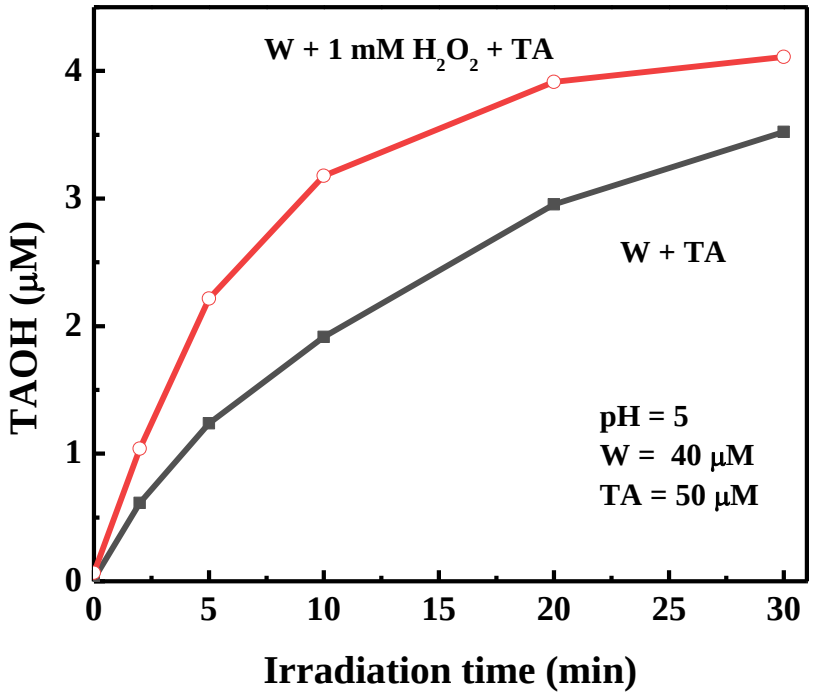
W + 1 mM H2O2 + TA
W + TA
pH = 5
W = 40 μM
TA = 50 μM
TAOH (μM)
Irradiation time (min)
0
1
2
3
4
0
5
10
15
20
25
30

555 **Figure 4**

556

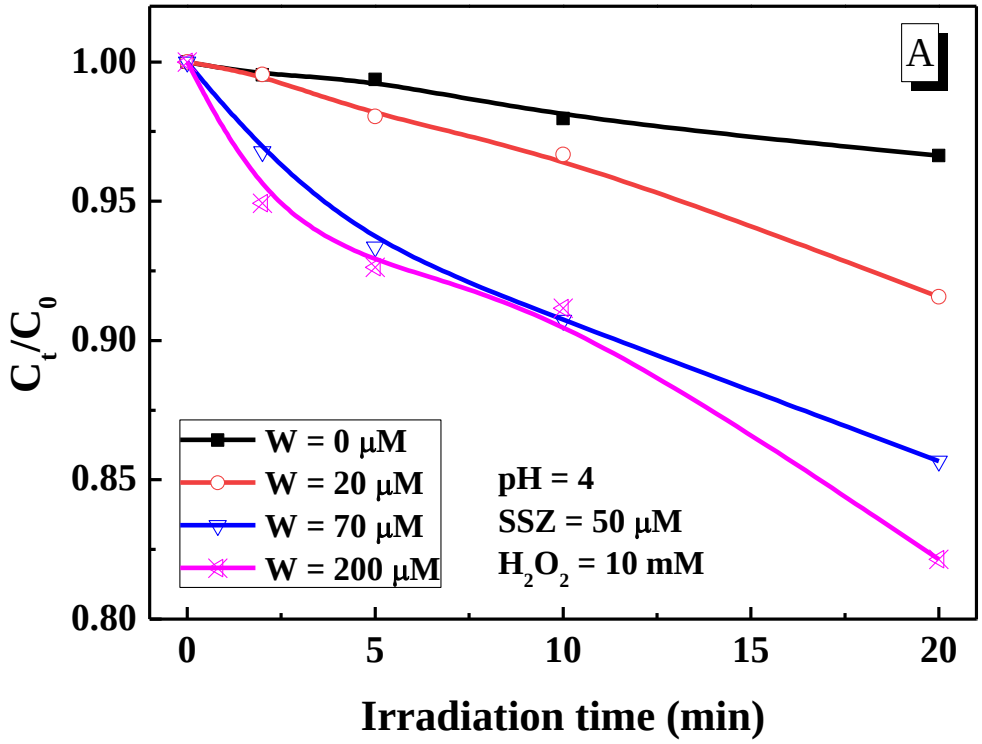

557

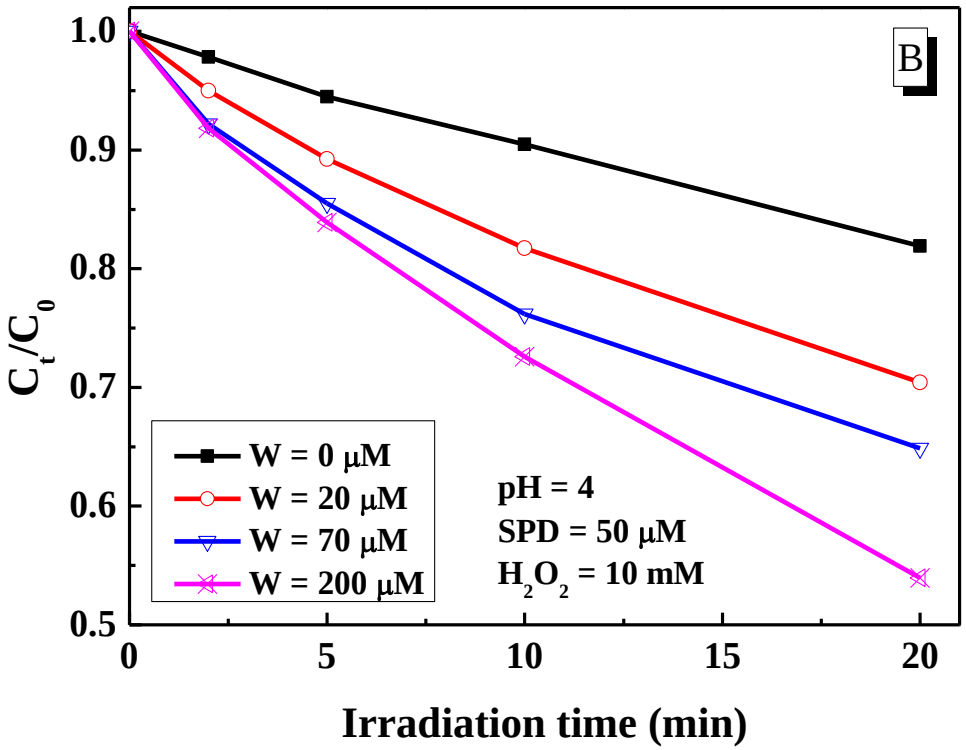

558

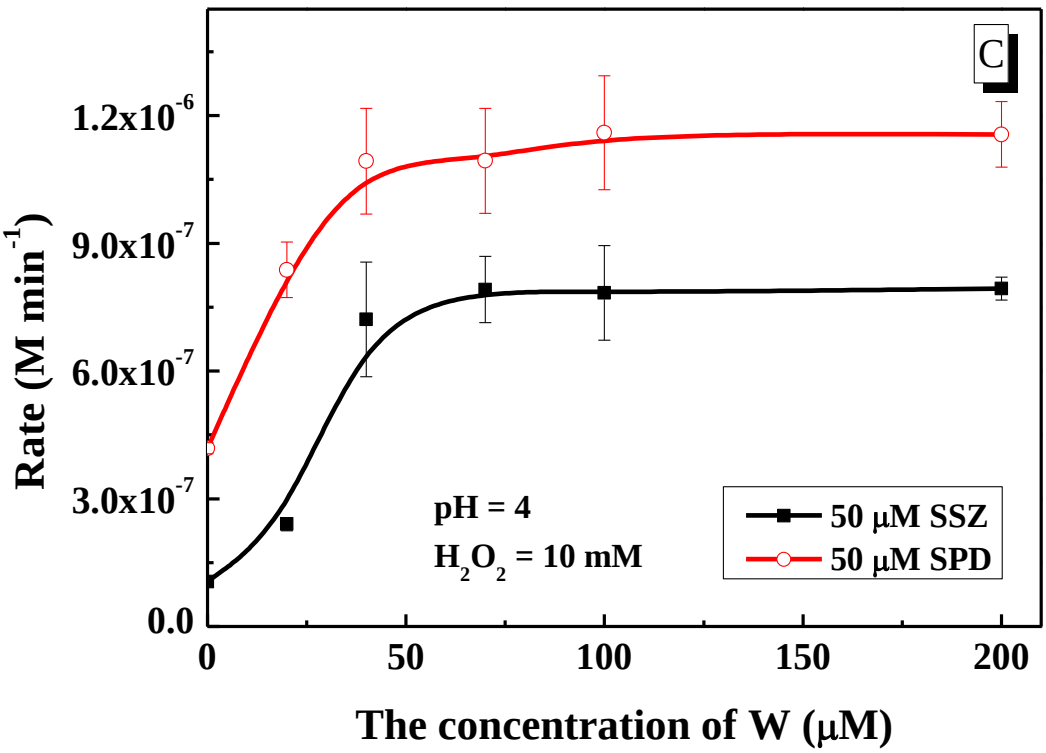
C
1.2x10-6
9.0x10-7
6.0x10-7
3.0x10-7
0.0
Rate (M min-1)
0
50
100
150
200
The concentration of W (μM)
pH = 4
H2O2 = 10 mM
50 μM SSZ
50 μM SPD

559

560

561

562 **Figure 5:**

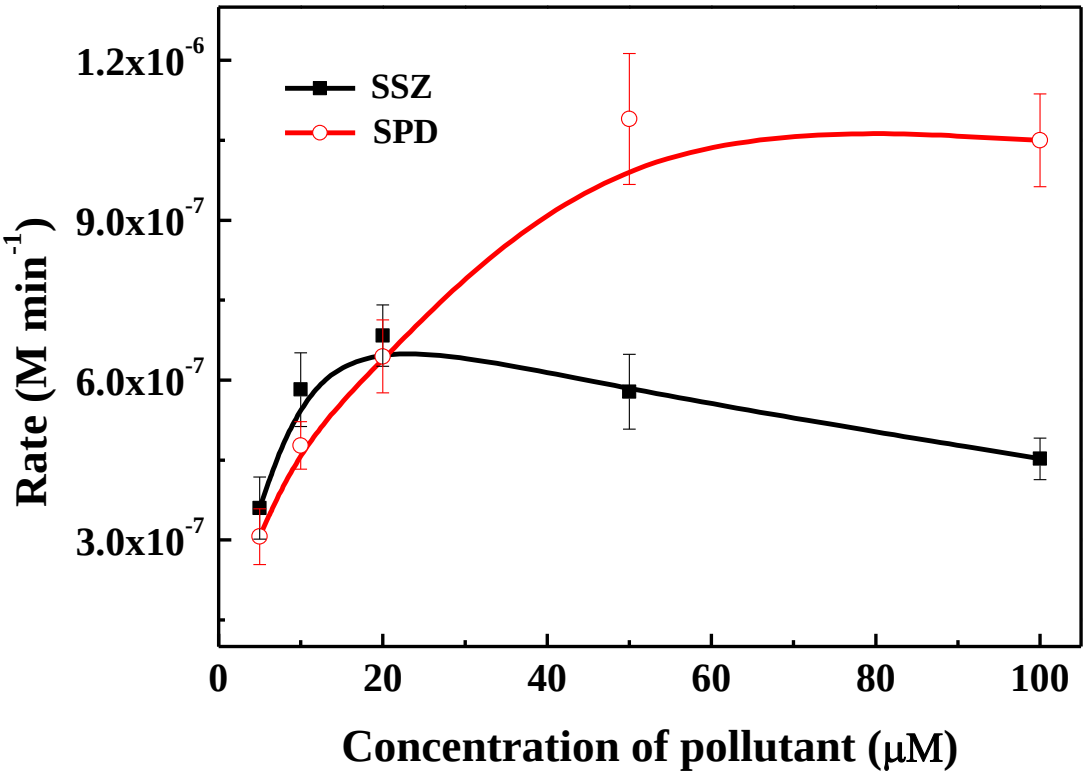

563

564

565

566 **Figure 6:**

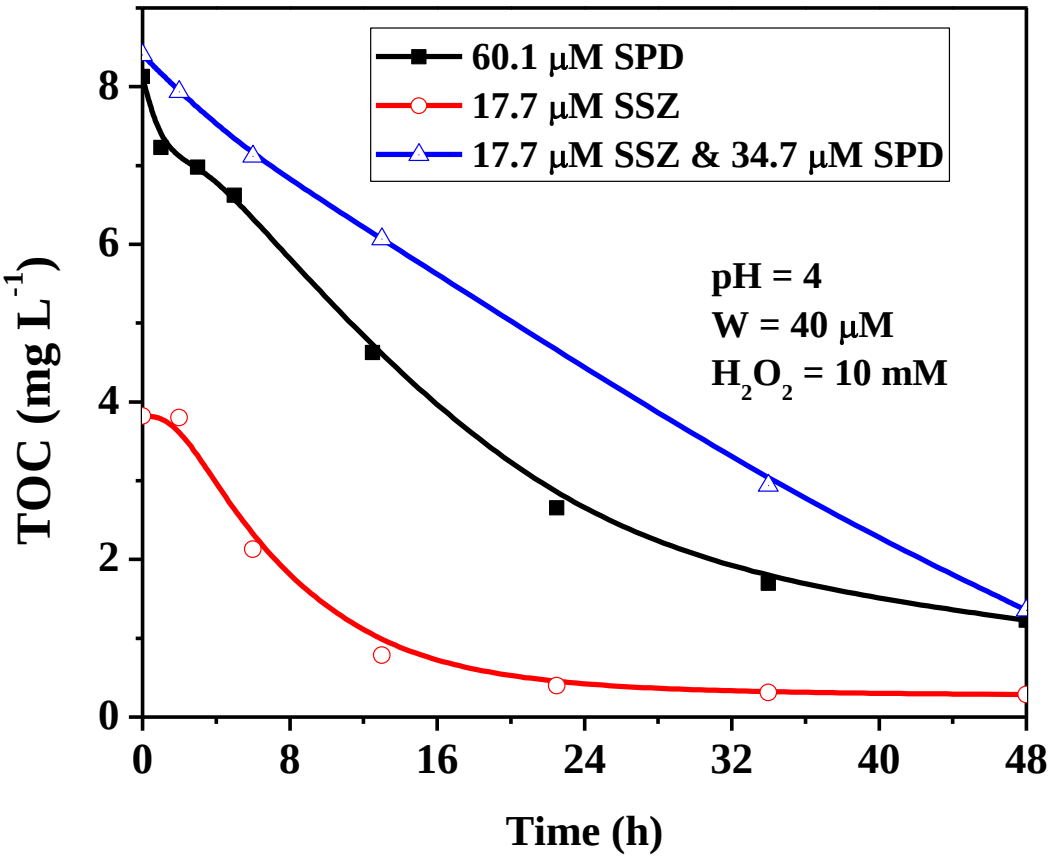

567
568

Table 1: SSZ and SPD initial degradation rates as a function of H_2O_2 concentration. [W] = 40 μM; [SSZ] = [SPD] = 50 μM; pH = 4.0.

[H_2O_2] mM	**Initial rate of SSZ disappearance M min^{-1}**		**Initial rate of SPD disappearance M min^{-1}**	
	Without decatungstate	**With decatungstate**	**Without decatungstate**	**With decatungstate**
0	No degradation	1.2×10^{-7}	No degradation	4.3×10^{-7}
1	0.1×10^{-7}	1.6×10^{-7}	0.6×10^{-7}	7.0×10^{-7}
10	1.1×10^{-7}	6.1×10^{-7}	4.2×10^{-7}	10.9×10^{-7}
50	5.0×10^{-7}	14.0×10^{-7}	13.7×10^{-7}	21.9×10^{-7}
100	7.2×10^{-7}	21.5×10^{-7}	21.3×10^{-7}	33.9×10^{-7}

Table 2: MS analysis of SPD and SSZ by-products and suggested structures. [W] = 40 µM; [H_2O_2] = 10 mM; [SSZ] = [SPD] = 50 µM; pH = 4.0.

SSZ			SPD		
m/z	**Elemental composition**	**Suggested structure**	**m/z**	**Elemental composition**	**Suggested structure**
398	$C_{18}H_{14}N_4O_5S$	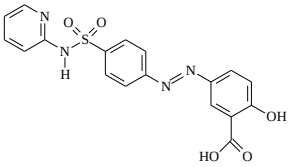	**249**	$C_{11}H_{11}N_3O_2S$	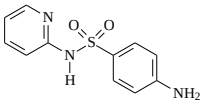
414	$C_{18}H_{14}N_4O_6S$	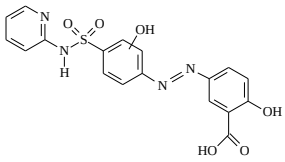	**250**	$C_{11}H_{10}N_2O_3S$	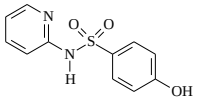
334	$C_{18}H_{14}N_4O_3$	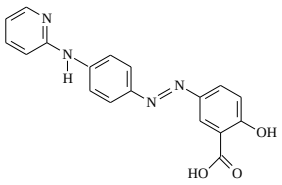	**281**	$C_{11}H_{11}N_3O_4S$	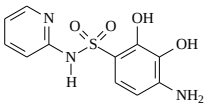
249	$C_{11}H_{11}N_3O_2S$	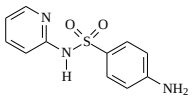	**265**	$C_{11}H_{11}N_3O_3S$	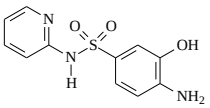
250	$C_{11}H_{10}N_2O_3S$	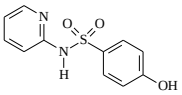	**263**	$C_{11}H_9N_3O_3S$	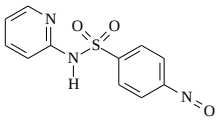
186	$C_{11}H_{10}N_2O$	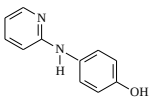	**279**	$C_{11}H_9N_3O_4S$	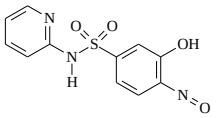
202	$C_{11}H_{10}N_2O_2$	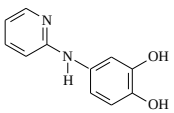	**266**	$C_{11}H_{10}N_2O_4S$	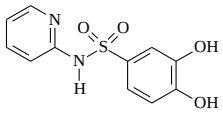
266	$C_{11}H_{10}N_2O_4S$	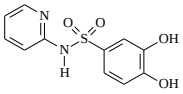	**185**	$C_{11}H_{11}N_3$	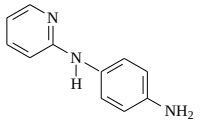

186	**$C_{11}H_{10}N_2O$**	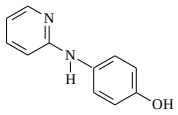
202	**$C_{11}H_{10}N_2O_2$**	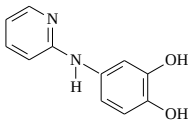

578
579